Measurements of biologically effective UV doses, total ozone abundances, and cloud effects with multichannel, moderate bandwidth filter instruments

Arne Dahlback

I describe a method to derive biologically effective UV dose rates, total ozone abundances, and cloud optical depths from irradiance measurements with moderate bandwidth filter instruments that have only a few channels in the UV region. These quantities are determined when the measured irradiances are combined with radiative transfer calculations. The method was applied to a four-channel filter instrument with center wavelengths at 305, 320, 340, and 380 nm and bandwidths of 10 nm. I compared the instrument with a high-wavelength-resolution spectroradiometer during a 1-week period in San Diego, California, with variable cloudiness. The relative difference in Commission Internationale de l'Éclairage (CIE)-weighted UV dose rates for solar zenith angle's (SZA's) $< 80°$ was $1.4 \pm 3.2\%$. The relative difference for clear sky was $0.6 \pm 1.5\%$ for SZA's $< 80°$. The total ozone inferred from the irradiance measurements with the filter instrument is insensitive to clouds. The instrument was compared with a Dobson and a Brewer instrument in Oslo, Norway, 60 °N, for more than 1 year. The relative difference in derived ozone abundance for the entire period, including cloudy days, was $0.3 \pm 2.9\%$. The standard deviation was reduced to 1.9% when only clear sky and SZA's $< 60°$ were included. By using the total ozone and the cloud optical depth derived from the filter instrument as input to a radiative transfer model, one can compute a complete spectrum from 290 to 400 nm with 1-nm resolution. Such calculated spectra are in good agreement with spectra measured simultaneously with a high-wavelength-resolution spectroradiometer for clear as well as cloudy sky conditions and can be used to determine dose rates for any desired action spectrum. Only one UV-B channel and one UV-A channel are required to compute the spectra.

Key words: UV radiation, UV doses, ozone, radiometer, cloud transmission.

1. Introduction

The spectral distribution of solar UV radiation reaching the Earth's surface depends on the radiation emitted by the Sun, the Earth–Sun separation, the optical properties of the atmosphere, the solar zenith angle (SZA), and the reflection properties of the Earth's surface. The transmission of solar radiation in the UV-B region (280–315 nm) through the stratosphere is primarily determined by the total amount of stratospheric ozone. In the troposphere the attenuation is due mainly to scattering by air molecules (Rayleigh scattering) and scattering in clouds (water or ice particles). Changes in tropospheric cloud cover can affect significantly UV penetration, but cloud cover variations are expected to influence UV-A (315–400 nm) and UV-B in much the same way because of the weak wavelength dependence of scattering in clouds. A decrease in total ozone abundance is expected generally to lead to an increase in harmful UV radiation if all other parameters are kept unchanged. Large increases in UV-B have been measured in association with the "ozone hole" at high southern latitudes. In 1993 erythemally weighted UV dose rates at Palmer Station, Antarctica (64.5 °S), sometimes exceeded the summer maximum in San Diego (32 °N).[1] A downward trend in total ozone in the Northern Hemisphere has been confirmed by satellite as well as by ground-based observations.[2] Kerr and McElroy[3] reported a significant increase in UV-B from 1989 to 1993 at Toronto

The author is with the Norwegian Institute for Air Research, P.O. Box 100, N-2007 Kjeller, Norway.

Received 21 November 1995; revised manuscript received 10 June 1996.

0003-6935/96/336514-08$10.00/0

(44 °N) caused by a decrease in total ozone during the same period.

Frederick *et al.*[4] noted that variability in cloudiness is among the largest sources of variance in monthly integrated UV irradiance at the ground. Therefore, to detect trends in solar UV-B radiation that are due to trends in total ozone, an UV monitoring network should measure UV radiation, total ozone, and cloud transmission. High-wavelength-resolution spectroradiometers can provide detailed information about the spectral distribution. Stamnes *et al.*[5] showed that spectra from such instruments can be used to determine total ozone and cloud transmission accurately. However, such instruments are expensive and require extensive labor in maintenance and calibration. To increase the geographic coverage in an UV monitoring network, simpler and less expensive instruments are needed. Single broadband instruments with an instrumental responsivity close to action spectra such as erythema are used widely. However, broadband instruments provide limited information because they cannot distinguish between variations in UV radiation caused by alteration in cloud cover and variations caused by changes in the total ozone abundance. Also, the data from such instruments cannot be converted to UV doses with an action spectrum different from the instrumental response. A compromise between single broadband instruments and spectroradiometers is multichannel instruments with channels in both the UV-B and the UV-A regions. In this paper I show that data from such instruments combined with radiative transfer calculations provide reliable data on biologically effective UV dose rates, total ozone abundance, and effective cloud optical depth or cloud transmission. Only two channels are required to determine these quantities. Furthermore, by using the derived total ozone abundance and the effective cloud optical depth as input to a radiative transfer model, one can compute a high-wavelength-resolution spectrum covering both the UV-B and the UV-A regions. Such computed spectra are in good agreement with measured spectra from a high-wavelength-resolution spectroradiometer. An additional advantage is that these spectra reconstructed from the multichannel measurements can be applied to a variety of different action spectra to predict any desired biological effect.

The optical part of a multichannel filter instrument consists typically of a Teflon or a quartz diffuser, interference filters, and photosensitive detectors. The methodology I describe in Sections 4–7 are applied to data from a GUV-511 instrument. The GUV-511, manufactured by Biospherical Instruments, San Diego, has four UV channels. The center wavelengths are approximately 305, 320, 340, and 380 nm and the bandwidths are approximately 10 nm FWHM. The instrument is temperature stabilized at 40 °C. The time resolution is normally 1–2 min. I note here that the methodology discussed in Sections 4–7 may work also on other multichannel filter instruments. The requirements are that the instrument has at least one channel in the UV-B region (sensitive to both ozone and clouds) and one channel in the UV-A region (sensitive to clouds but not to ozone). Furthermore, the relative responsivity for each channel as a function of wavelength must be known.

2. Radiative Transfer Model

The UV radiation model used here is based on the discrete ordinate solution to the radiative transfer equation[6] and is modified to include the curvature of the atmosphere,[7] which is necessary for large SZA's. The model includes all orders of multiple scattering and absorption, and the ground is treated as a Lambertian reflector. The optical properties are allowed to vary vertically. The atmosphere is divided into a suitable number of layers to resolve the optical properties adequately. The model includes molecular (Rayleigh) scattering as well as scattering and absorption by clouds. The ozone cross sections are taken from Ref. 8 and the Rayleigh-scattering cross sections are calculated with an empirical formula.[9] A parametric scheme[10] was used to model the clouds. The extraterrestrial solar spectrum is taken from Ref. 11 and has 1-nm wavelength resolution.

3. Calibration of Multichannel Instruments

The absolute spectral responsivity of a channel denoted by i can be described by a function $R_i(\lambda)$, where λ is the wavelength. The voltage V_i across the detector in channel i that is due to illumination by radiation with spectral irradiance $F(\lambda)$ can be described by

$$V_i = \int_0^\infty R_i(\lambda) F(\lambda) \mathrm{d}\lambda. \tag{1}$$

One can calibrate each channel in the filter instrument in absolute units (i.e., $\mathrm{W/m^2\ nm}$) by placing the instrument in front of a calibration lamp under conditions specified by the National Institute of Standards and Technology.[12] The output voltage V_i in channel i can be related to the irradiance at a certain wavelength by the introduction of a calibration constant C_i that can be determined by $C_i = V_i/F_{\mathrm{lamp}}(\lambda)$,[13] where λ is the center wavelength of $R_i(\lambda)$. However, the shape of the lamp spectrum (usually a 1000-W FEL lamp) is different from the solar spectrum. Booth *et al.*[13] showed that this difference will lead to an error in the measured irradiance of solar radiation for a channel with a center wavelength of 305 nm and a bandwidth of 10 nm FWHM of approximately 75% relative to a high-wavelength-resolution spectroradiometer. Booth *et al.* also showed that using the Sun as the calibration source instead of a FEL lamp will reduce the errors considerably. However, the shape of the solar spectrum at the surface, and hence the spectral distribution of $R_i(\lambda)F(\lambda)$ in Eq. (1) will change with the SZA or the total ozone abundance. To demonstrate this, the spectral distribution of $R_i(\lambda)F(\lambda)$ for a channel with a center wavelength of 305 nm and a bandwidth of 10 nm FWHM was calculated for different ozone

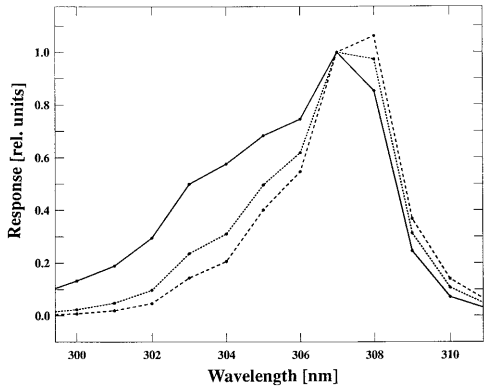

Fig. 1. Spectral distribution $R(\lambda)F(\lambda)$ in the UV-B channel with a center wavelength of 305 nm and a bandwidth of 10 nm FWHM varies with total ozone abundance and SZA. $R(\lambda)F(\lambda)$ was calculated for SZA = 0°, 300 DU (solid curve); SZA = 60°, 300 DU (dotted curve); and SZA = 60°, 400 DU (dashed curve).

abundances and SZA's as shown in Fig. 1. Therefore the error in measured irradiance with such a channel relative to a high-wavelength-resolution spectroradiometer depends on how much the atmospheric conditions during the measurement differ from the atmospheric conditions at the time of calibration.

As shown later, we do not need a calibration factor related to a certain wavelength as described above. The quantity we need is the absolute responsivity for each channel $R_i(\lambda)$ defined in Eq. (1). I now describe how $R_i(\lambda)$ can be determined if the relative responsivity $R_i'(\lambda)$ is known. The relation between the relative and absolute responsivity can be written as

$$R_i(\lambda) = k_i R_i'(\lambda), \tag{2}$$

where k_i is a channel and instrument-dependent constant. The absolute responsivity $R_i(\lambda)$ can be determined if the constant k_i is known. By combining Eqs. (1) and (2) we can express k_i as

$$k_i = \frac{V_i}{\int_0^\infty R_i'(\lambda)F(\lambda)\mathrm{d}\lambda} = \frac{V_i}{\sum_{\lambda=0}^{\infty} R_{i\lambda}'F_\lambda \Delta\lambda}, \tag{3}$$

where V_i is the voltage across channel i in the filter instrument, and $F(\lambda)$ is the spectrum measured simultaneously with a spectroradiometer. The light source can be either a calibration lamp or the Sun. If the Sun is used as a calibration source, the measurement should be performed around local noon when the sky is clear and the Sun is high in the sky. This will ensure that the spectrum will not change during the scan time. Note that we need only one spectrum from the spectroradiometer to calibrate all channels of the filter instrument. Also note that the calibration of the filter instrument is only as good as the reference spectroradiometer.

4. Biologically Effective UV Doses

To determine the UV dose rate, labeled D instead of $\mathrm{d}D/\mathrm{d}t$ for simplicity, from a spectroradiometer, we need to convolve the spectral irradiance $F(\lambda)$ with a biological action spectrum $A(\lambda)$:

$$D_{\text{exact}} = \int_0^\infty A(\lambda)F(\lambda)\,\mathrm{d}\lambda = \sum_{\lambda=0}^{\infty} A_\lambda F_\lambda \Delta\lambda, \tag{4}$$

where $\Delta\lambda$ is determined by the resolution of the spectroradiometer. The UV dose is a time-integrated quantity and is obtained when we integrate the UV dose rate over a specified time interval. A multichannel filter instrument, however, has only a few channels M available in the UV part of the spectrum. Now we attempt to determine the UV dose rate by a linear combination of the irradiances (represented by the voltages V_i) measured by the M channels. For a filter instrument having M channels,

$$D_{\text{approx}} = \sum_{i=1}^{M} a_i V_i. \tag{5}$$

The goal is to determine a unique set of these M coefficients a_i's. Thus we try to determine accurate dose rates for a specified action spectrum for all realistic atmospheric conditions (primarily variable ozone amount, ozone profile, SZA, cloud cover, and surface albedo) by using one single set of a_i's in Eq. (5). We proceed by requiring that the accurate expression for the dose rate [Eq. (4)] equals the approximate dose rate [Eq. (5)], i.e., $D_{\text{exact}} = D_{\text{approx}}$:

$$\sum_{i=1}^{M} a_i V_i = \sum_{\lambda=0}^{\infty} A_\lambda F_\lambda \Delta\lambda. \tag{6}$$

We need a set of M equations to obtain a solution of the M unknowns a_i. In principle, this can be obtained by simultaneous measurements with a spectroradiometer and the filter instrument at M different solar conditions. However, instead we use the radiative transfer model to compute the M spectra necessary to solve Eq. (6). By inserting Eq. (3) into Eq. (6), we obtain

$$\sum_{i=1}^{M} a_i k_i \sum_{\lambda=0}^{\infty} R_{i\lambda}'F_\lambda = \sum_{\lambda=0}^{\infty} A_\lambda F_\lambda. \tag{7}$$

The a_i's will depend on the chosen action spectrum. Furthermore, they will (at least partly) also account for the parts of the spectrum that contribute to the dose rate but are not measured by the filter instrument. The accuracy of the dose rates determined with the filter instrument with these a_i's will in general depend on the action spectrum A, the number of channels M, and at what wavelengths the channels are located. Furthermore, the accuracy will depend also on the spectra F_λ chosen in Eq. (7) to solve for the a_i's. It is beyond the scope of this paper to discuss this further. Instead, I focus on the GUV-511 instrument that has four channels centered at 305, 320, 340, and 380 nm with a bandwidth of 10 nm FWHM. I choose the action spectrum A to be the widely used Commission International de l'Éclairage (CIE) action spectrum.[14] With four channels we need four different spectra to solve for the four a_i's in Eq. (7). I

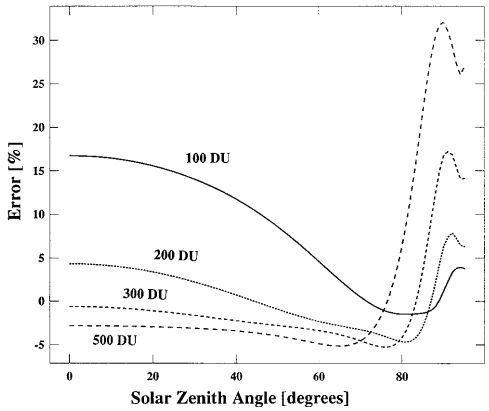

Fig. 2. Approximate UV dose rate [D_{approx} in Eq. (5)] for the GUV-511 instrument is sensitive to ozone only for small ozone abundances in combination with small SZA's and large ozone abundances in combination with large SZA's. The error ε defined by $[(D_{exact} - D_{approx})/D_{exact}]$ was calculated as a function of a SZA $< 90°$ and total ozone abundances $\Omega = 100$–500 DU.

computed the four spectra needed for a clear atmosphere by using two different ozone amounts [320 and 340 Dobson units (DU)] and two different SZA's (40° and 60°). The ground albedo A_g was set to 0.0. To get an idea of how accurately the UV dose rates can be determined with the four a_i's, D_{approx} (simulating the GUV-511) and D_{exact} (simulating a spectroradiometer with wavelength resolution of 1 nm) were calculated for a large variety of combinations of SZA's ranging from 0° to 80°, cloud optical depths τ from 0 to 60, and ozone amounts from 200 to 500 DU. This resulted in an error defined by $100\,[(D_{exact} - D_{approx})/D_{exact}]$ in the simulated dose rate less than 5%. Larger errors are found for small ozone abundances in combination with small SZA's and for large ozone abundances in combination with large SZA's. This is demonstrated in Fig. 2 where the error is shown for 100, 200, 300 and 500 DU for $0° < \text{SZA} < 90°$, all calculated for clear sky. Because the total ozone amount Ω can be determined from the GUV-511 measurements (see below), we can reduce the error of D_{approx} by introducing an error function ε(Ω, SZA) in Eq. (5):

$$D_{approx}^{corrected} = [1 + \varepsilon(\Omega, \text{SZA})]D_{approx}, \qquad (8)$$

where $\varepsilon(\Omega, \text{SZA}) = [(D_{exact} - D_{approx})/D_{approx}]$ is the error function shown in Fig. 2.

The GUV-511 was run side by side with a high-wavelength-resolution spectroradiometer in San Diego from 24 July to 1 August 1993. The spectroradiometer, an SUV-100, is similar to the instruments used at the National Science Foundation UV monitoring network in southern and northern polar regions.[1] Scans from 280 to 600 nm were taken every 30 min during the period. The GUV-511 was operated continuously in a 2–min average mode. I determined the absolute response functions for each of the four channels as explained above by using one spectrum measured on a clear day at noon

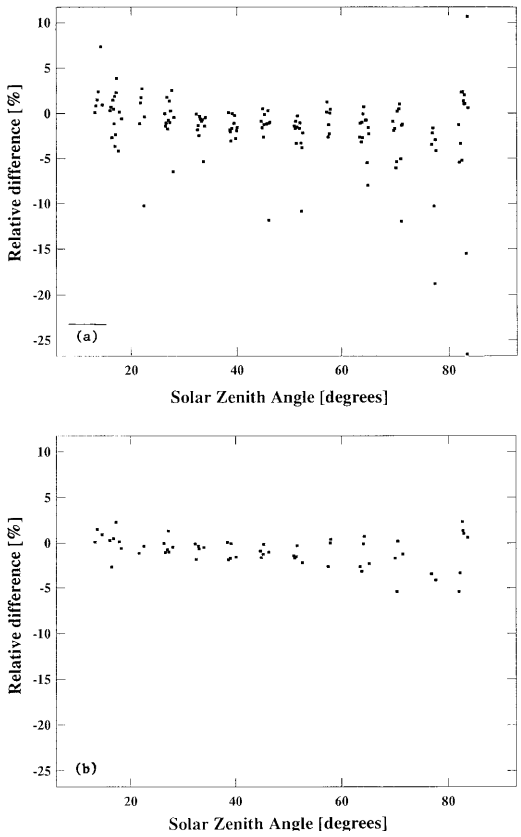

Fig. 3. Comparison of CIE-weighted UV dose rates determined with the GUV-511 instrument and the SUV-100 spectroradiometer in San Diego for the period from 24 July to 1 August 1993 shown as 100(SUV-GUV)/SUV. (a) all data (variable cloud cover); (b) only data close to clear sky ($\tau < 10$).

by the SUV-100 [24 July, 20 h Coordinated Universal Time (UTC)]. I determined the CIE-weighted UV dose rates $D_{approx}^{corrected}$ from the GUV-511 measurements with Eqs. (5) and (8). ε in Eq. (8) was interpolated from a lookup table. I calculated accurate dose rates D_{exact} with the SUV-100 spectra in Eq. (4). The percentage difference $100(D_{exact} - D_{approx}^{corrected})/D_{exact}$ as a function of SZA's is shown in Figs. 3(a) and 3(b). In Fig. 3(a) all measurements are included, whereas in Fig. 3(b) only those for which the cloud optical depth was less than 10 are included. In Fig. 3(a) the average percentage difference is −1.4%, and the standard deviation is 3.2% for SZA's $< 80°$. For the near-clear-sky cases in Fig. 3(b), the average difference is −0.6%, and the standard deviation is 1.5% for all SZA's $< 80°$. The reason for the somewhat larger discrepancy between the SUV-100 and the GUV-511 in Fig. 3(a) is probably partly because the measurements were not carried out in exactly the same time period, so drifting clouds may have affected the GUV-511 and the SUV-100 differently.

The coefficients a_i that were used to determine the dose rates in the above example were calculated with the radiative transfer model with a mid-latitude model atmosphere[15] for clear sky and a ground albedo

$A_g = 0.05$. However, the vertical distribution of ozone and the ground albedo can change considerably, especially at high latitudes. I tested the sensitivity to the ozone profile by calculating the coefficients a_i for two very different atmospheric profiles: a Tropical Standard and a Subarctic Winter Standard.[16] All the GUV-511 dose rates from the San Diego intercomparison were recalculated with these two new sets of a_i's. For all SZA's $< 85°$, the change in dose rates was found to be less than 0.3%, which shows that a unique set of a_i's can be used for all realistic ozone profiles. I tested the sensitivity to ground albedo A_g by calculating the a_i's for $A_g = 0.9$ and for $A_g = 0.0$. This resulted in a change in all the GUV-511 dose rates $< 1.0\%$ for all ZSA's $< 85°$. Thus the use of a unique set of a_i's will lead only to small errors if the surface albedo varies. From the above discussion and the comparison of the SUV-100 dose rates with the GUV-511 dose rates, it can be concluded that only one single set of a_i's is needed to determine CIE-weighted UV dose rates accurately for the GUV-511 for all realistic atmospheric conditions and surface albedo.

5. Total Ozone

It is well established that total ozone abundances can be accurately and reliably determined from spectral global UV irradiance measurements by a comparison of measured N values, defined by $N = F_{\lambda'}/F_{\lambda}$ to N values computed from a comprehensive radiative transfer model.[5] λ' and λ are wavelengths for which the ozone absorption cross sections are very different. This can be generalized to instruments such as the GUV-511 if the response functions are included in the definition of the N values as

$$N = V_i/V_j = \left(\sum_{\lambda=0}^{\infty} R_{i\lambda}F_{\lambda}\right)/\left(\sum_{\lambda=0}^{\infty} R_{j\lambda}F_{\lambda}\right), \qquad (9)$$

where i and j refer to two different channels in the multichannel instrument that have different ozone absorption cross sections. Stamnes *et al.*[5] showed that the spectral irradiance ratio was insensitive to clouds for $\lambda' = 340$ nm and $\lambda = 305$ nm. If the filter instrument has more than two channels available, several wavelength pairs can be used. The GUV-511 has four channels available, namely, the 305-, 320-, 340-, and 380-nm channels. The 305-nm channel is sensitive to ozone variations and can be combined with one of the other three channels to form an N value. Computer simulations show that the least influence of clouds on the derived total ozone abundance is obtained with the 320:305 ratio. Simulations show that a cloud layer between 2 and 4 km with optical depth $\tau = 100$ introduces an error of less than 2 DU for all SZA's if N values based on clear sky and surface albedo $A_g = 0.0$ are used to infer the total ozone abundance. The corresponding error for the 340:305 ratio is 5 DU. However, the error increases with the surface albedo. For a surface albedo $A_g = 0.8$, the error for the 320:305 ratio increases to 20 DU for a cloud layer between 2 and 4 km with cloud optical depth $\tau = 100$. The reason for this larger error can be explained by a multiple reflection between the cloud base and the surface leading to an increased path length for the radiation and thus increased absorption. The denominator in Eq. (9) will thus decrease, leading to an increase in the N value and this will be interpreted as an increase in the total ozone abundance compared with the clear-sky case. To save computer time, the radiative transfer model was used to compute N values defined by Eq. (9) for a variety of SZA's and ozone abundances to create a lookup table from which the total ozone abundance is determined when measured ratios are compared with the computed ratios.

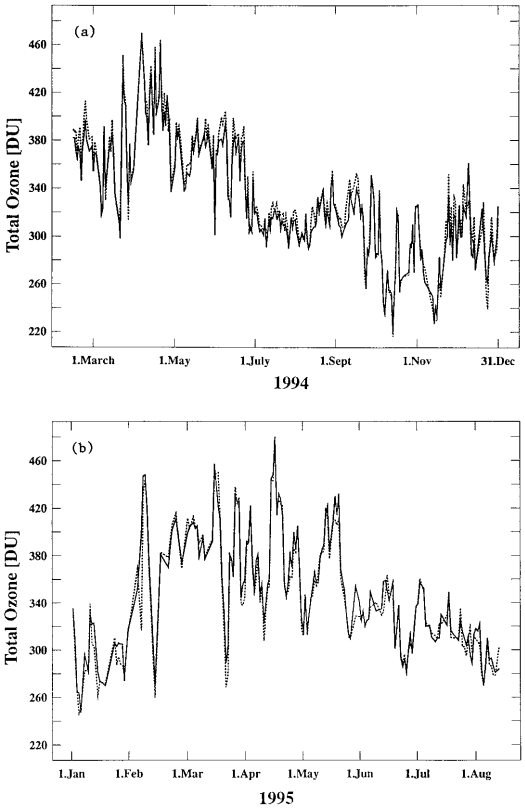

Fig. 4. Comparison of daily total ozone abundance from the GUV-511 (dotted curve) and Dobson 56 and Brewer 42 instruments (solid curves) in Oslo, Norway (60 °N), for the period from 15 February 1994 to 20 August 1995. The data contain clear as well as cloudy days. (a) 1994 data; (b) 1995 data.

Total ozone derived from measurements with a GUV-511 was compared with daily total ozone based on measurements with the Dobson 56 and the Brewer 42 instruments in Oslo, Norway (60 °N), during the period 15 February 1994 to 14 August 1995 as shown in Figs. 4(a) and 4(b). The average percentage difference for the period, defined by 100 (Dobson-GUV)/Dobson, is -0.3% and the standard deviation is 2.9%. The measurements include cloudy as well as clear-sky cases. The SZA at local noon is 83° in December and 36° in June. If we consider only clear-sky cases for March–September (representing a time of the

year with high Sun—a SZA $< 60°$), the standard deviation is smaller at 1.9%.

To investigate the influence of the ozone profile on the N values, I computed lookup tables for two very different ozone profiles: a Subarctic Winter profile and a Tropical profile.[16] For SZA's $< 60°$, the percentage difference in calculated ozone is less than 1%. The difference increases with SZA and is 3% at 70° and 30% at 80°. Therefore the choice of ozone profile in the calculations of the N values used in the lookup table is important for this station only in the winter but of little importance in the summer. It was found that total ozone derived from N values based on a mid-latitude ozone profile[15] agrees well with Dobson values in Oslo during the wintertime.

6. Cloud Optical Depths

Clouds have a strong influence on UV attenuation both in the UV-A and the UV-B regions, and the wavelength dependence is weak. Radiation in the UV-A region, however, is nearly insensitive to ozone. Stamnes *et al.*[5,17] showed that spectral measurements in the UV-A region combined with radiative transfer calculations can be used to infer cloud optical depths. They used their radiative transfer model (basically the same model as used here) to compute the spectral irradiance F_λ. They determined the cloud optical depth by computing F_λ for various cloud optical depths until the model that calculated F_λ agreed with the measured F_λ. The authors also noted that the inferred cloud optical depth is model dependent and must be interpreted as the optical depth of a stratified cloud layer inserted in the model that makes the computed spectral irradiance agree with the measured irradiance at the same wavelength. This means that if the real ground albedo differs from the ground albedo used in the model, the radiative effect that is due to this difference is absorbed in our definition of cloud optical depth. Their procedure for determining cloud optical depths can be applied to measurements with filter instruments if the voltage V_i in Eq. (1), across the selected channel in the UV-A, is computed for various cloud optical depths until the measured and computed values of V_i agree. An illustration of the influence of clouds on the CIE-weighted UV dose rate during one day is provided in Fig. 5, where the dose rate as well as the cloud optical depth are shown as a function of time on 10 October 1992. The figure demonstrates the clear anticorrelation between the dose rate and cloud optical depth. The 380-nm channel in the GUV-511 was used to determine the cloud optical depth.

Alternatively, the cloud effect on UV radiation could be characterized by a simple ratio, which is the irradiance actually received at the ground divided by the irradiance that would have existed under clear skies. However, the advantage of one deriving an effective cloud optical depth is that this quantity can be used as input to the radiation model to reconstruct spectra as explained in Section 7.

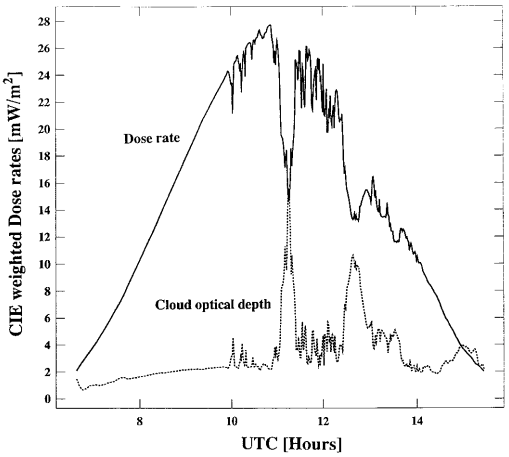

Fig. 5. CIE-weighted UV dose rates and cloud optical depths measured with a GUV-511 instrument on 10 October 1992 in Oslo. This demonstrates the clear anticorrelation between dose rate and cloud optical depth.

7. Reconstructed Spectra

The most important factors controlling the attenuation of solar UV radiation are the solar elevation, the total ozone abundance, cloud cover, and the ground albedo. Both the total ozone amount and the effective cloud optical depth can be determined from the measured irradiances as explained in the previous sections. Using the total ozone value and the effective cloud optical depth derived from measurements with the multichannel filter instrument as input to the radiative transfer model, we can compute realistic spectra. Figures 6(a) and 6(b) show two such quasi-measured spectra (one clear-sky case and one case with overcast sky) from the GUV-511, as well as simultaneous measured spectra with the SUV-100. The UV-B region is shown in Fig. 6(a) and the UV-A region in Fig. 6(b). The spectra were measured in San Diego at 20.08 UTC, 24 July 1993 (total ozone 296 DU, SZA = 13.3°, and equivalent stratified cloud optical depth $\tau = 5.3$ representing clear sky) and at 20.08 UTC, 25 July 1993 (total ozone 294 DU, SZA = 13.5°, and $\tau = 32.1$ representing cloudy sky). The agreement between the calculated spectrum (based on GUV-511 measurements) and the spectrum measured with the SUV-100 is good in both the UV-B region and the UV-A region. The structure of the SUV-100 spectra does not match the spectra inferred from the GUV-511 measurements partly because the center wavelengths differ by 0.2 nm in the UV-B and 0.3 nm in the UV-A. Also, a spectrum measured with a spectroradiometer depends on the slit functions in the instrument.[18] A better agreement in the spectral patterns would be obtained if the extraterrestrial spectrum used in the model was based on the one that would have been measured with the SUV-100 outside the atmosphere or inferred from a Langley plot.

If the actual ground albedo is lower than the ground albedo used in the model, the actual clear-sky irradiance would be lower than the model clear-sky

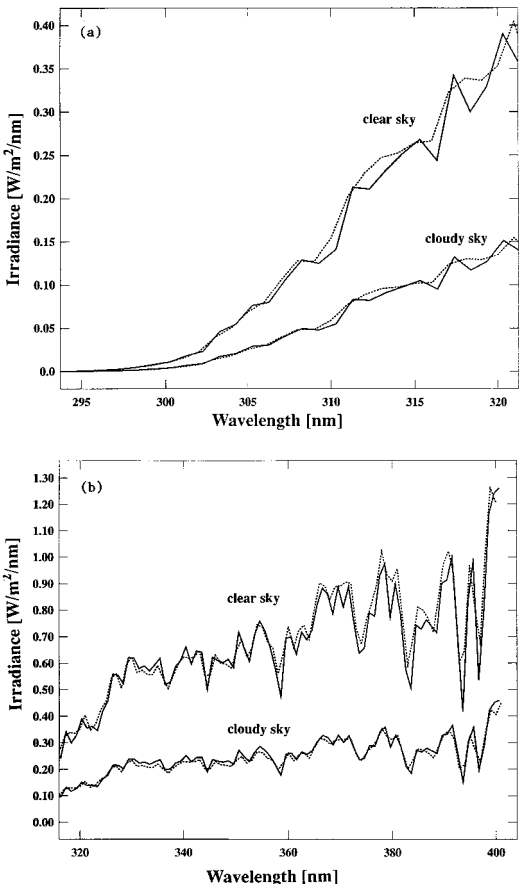

Fig. 6. Comparison of calculated spectra based on derived ozone and cloud optical depth from measurements with GUV-511 (solid curves) and simultaneously measured spectra with SUV-100 (dashed curves) spectroradiometer in San Diego. Both a clear-sky case (τ = 5.3, 296 DU, 20.08 UTC, 24 July 1994) and a cloudy-sky case (τ = 32.1, 294 DU, 20.08 UTC, 25 July 1993) are shown. (a) UV-B region; (b) UV-A region.

irradiance at the same wavelength. One can use the model to compensate for this by introducing an equivalent stratified cloud layer such that the modeled irradiance agrees with the actual clear-sky irradiance. The model ground albedo was set to 0.2. A more realistic value for bare ground would probably be closer to zero.[19] This partly explains why the derived effective cloud optical depth for the clear-sky case in Figs. 6(a) and 6(b) was 5.3 and not closer to zero as expected. If the spectral irradiance of the extraterrestrial spectrum used in the model[11] is too high, this will also partly explain the unexpected high effective cloud optical depth for the clear-sky case.

8. Conclusions

I described a method to derive biologically effective UV doses, total ozone abundances, and cloud optical depths or cloud transmissions from irradiance measurements with multichannel, moderate bandwidth filter-instruments. The absolute responsivity function has been determined for each channel by a comparison with a simultaneously measured spectrum obtained from a high-wavelength-resolution spectroradiometer. The UV dose-rate was determined by a linear combination of the irradiance measurements from the filter instrument. The coefficients in the linear combination depend on the action spectrum chosen, and they also account for the parts of the spectrum that contribute to the UV dose rate but that are not measured by the filter instrument. A unique set of coefficients can be obtained that is sufficient for accurate determination of UV dose rates for all realistic atmospheric conditions. I applied the method to a four-channel filter instrument with 10-nm bandwidths. Comparison with data from a high-wavelength-resolution spectroradiometer shows that the UV dose rates inferred from the filter instrument are in good agreement with those inferred from spectral measurements obtained by the spectroradiometer for cloudy as well as clear-sky conditions. Stamnes *et al.*[5] described a method to derive total abundance from measured spectral irradiance ratios. This method has been extended to channels with larger bandwidths by taking into account the responsivity function in the channels used. The inferred ozone value is insensitive to clouds. The four-channel filter instrument has been compared with a Dobson and a Brewer instrument for more than one year. The agreement between ozone values is good for at least all SZA's $< 83°$ and for clear as well as cloudy skies. Stamnes *et al.*[5] also described a method to determine equivalent stratified cloud optical depths from spectral UV-A irradiances. This method was extended to apply to moderate bandwidth UV-A channels by taking into account the channels responsivity function. A complete spectrum from 290 to 400 nm can be calculated with the inferred total ozone abundance and the equivalent stratified cloud optical depth as input to a radiative transfer model. Such quasi-measured spectra are in good agreement with spectra measured by a high-wavelength-resolution spectroradiometer for clear-sky as well as cloudy-sky conditions and can be applied to determine dose rates for any desired action spectrum. Only two channels are used to determine the total ozone abundance (one UV-B channel and one UV-A channel), and the same UV-A channel can be used to determine the equivalent stratified cloud optical depth. Thus only two channels are required for the determination of accurate spectra from measurements with a filter instrument.

The author thanks Finn Tønnessen and Søren H. H. Larsen, University of Oslo, Norway, for the use of their total ozone data and Charles R. Booth for the use of his SUV-100 data. This research was supported by the Norwegian Ministry of Environment and the Norwegian Research Council.

References

1. C. R. Booth, T. B. Lucas, T. Mestechkina, J. R. Tusson, IV, D. A. Neuschuler, and J. H. Morrow, *NSF Polar Programs UV Spectroradiometer Network 1993-1994 Operations Report* (National Science Foundation, Washington, D.C., 1995).
2. World Meteorological Organisation, *Scientific Assessment of Ozone Depletion: 1994*. WMO Global Ozone Monitoring

Project, report 37 (World Meteorological Organisation, Geneva, 1994).
3. J. B. Kerr and C. T. McElroy, "Evidence for large upward trends of ultraviolet-B radiation linked to ozone depletion," Science **262,** 1032–1034 (1993).
4. J. E. Frederick, P. F. Soulen, S. B. Diaz, I. Smolskaia, C. R. Booth, T. Lucas, and D. Neuschuler, "Solar ultraviolet irradiance observed from Southern Argentina: September 1990 to March 1991," J. Geophys. Res. **98,** D5, 8891–8897 (1993).
5. K. Stamnes, J. Slusser, and M. Bowen, "Derivation of total ozone abundance and cloud effects from spectral irradiance measurements," Appl. Opt. **30,** 4418–4426 (1991).
6. K. Stamnes, S.-C. Tsay, W. J. Wiscombe, and K. Jayaweera, "Numerically stable algorithm for discrete-ordinate-method radiative transfer in multiple scattering and emitting layered media," Appl. Opt. **27,** 2502–2509 (1988).
7. A. Dahlback and K. Stamnes, "A new spherical model for computing the radiation field available for photolysis and heating at twilight," Planet. Space Sci. **39,** 671–683 (1991).
8. R. J. Paur and A. M. Bass, "The ultraviolet cross-sections of ozone. II. Results and temperature dependence," in *Atmospheric Ozone*, Proceedings of the Quadrennial Ozone Symposium, Halkidiki, Greece (Reidel, Hingham, Mass., 1985), pp. 611–616.
9. M. Nicolet, "On the molcular scattering in the terrestrial atmosphere. An empirical formula for its calculation in the homosphere," Planet. Space Sci. **32,** 1467–1468 (1984).
10. Y. X. Hu and K. Stamnes, "An accurate parameterization of the radiative properties of water clouds suitable for use in climate models," J. Climate **6,** 728–742 (1993).
11. M. Nicolet, "Solar spectral irradiances with their diversity between 120 and 900 nm," Planet. Space Sci. **37,** 1249–1289 (1989).
12. J. H. Walker, R. D. Saunders, J. K. Jackson, and D. A. McSparron, *Spectral Irradiance Calibration*. Natl. Bur. Stand. Special Pub. 230-20 (U.S. Department of Commerce, Washington, D.C., 1987).
13. C. R. Booth, T. Mestechnica, and J. H. Morrow, "Errors in the reporting of solar spectral irradiance using moderate bandwidth radiometers and experimental investigation," in *Ocean Optics XII*, J. S. Jaffe, ed. Proc. SPIE **2258,** 654–663 (1994).
14. A. F. McKinlay and B. L. Diffey, "A reference action spectrum for ultra-violet induced erythema in human skin," in *Human Exposure to Ultraviolet Radiation: Risks and Regulations*, W. R. Passchler and B. F. M. Bosnajakovic, eds. (Elsevier, Amsterdam, 1987), pp. 83–87.
15. U.S. Standard Atmosphere 1976, National Oceanic and Atmospheric Administration, National Aeronautics and Space Administration, U.S. Air Force (GPO, Washington, D.C., 1976).
16. G. P. Anderson, S. A. Clough, F. X. Kneizys, J. H. Chetwynd, and E. P. Shettle, "AFGL atmospheric constituent profiles (0–120 km)," AFGL-TR-86-0110 Air Force Geophysics Laboratory, Hanscom Air Force Base, Mass., 1987.
17. K. Stamnes, Z. Jin, and J. Slusser, "Several-fold enhancement of biologically effective ultraviolet radiation levels at McMurdo Station Antarctica during the 1990 ozone 'hole'," Geophys. Res. Lett. **19,** 1013–1016 (1992).
18. B. G. Gardiner and P. J. Kirsch, "Setting standards for European ultraviolet spectroradiometers," Air pollution research report 53. European Commission. Directorate-General XII, Science, Research, and Development, L-2920 Luxembourg, Report EUR 16153 (1995).
19. S. Madronich, "The atmosphere and UV-B radiation at ground level," in *Environmental UV Photobiology*, A. R. Young, L. O. Bjorn, J. Moan, and W. Nultsch, eds. (Plenum, New York, 1993).